

STABILITY ANALYSIS FOR A VERY FLEXIBLE FLYING

Liu Yi¹, Xie Changchuan², Xu Yuntao¹, Zhou Danjie¹

¹ Beijing Electro-Mechanical Engineering Institute
Liuyibuaa@126.com

² School of Aeronautics Science and Engineering, Beihang University,
Key Laboratory of Aircraft Advanced Design Technology (Beihang University),
xiechangc@163.com

Keywords: nonlinear coupled stability, flight dynamics, aeroelasticity, flexible flying wing

Abstract: A theoretical analysis model is established to simultaneously investigate the flight dynamics and aeroelastic stability of the flexible flying wing. The coupling effects between the rigid motion and structural elastic motion tend to be significant and strongly affect the aircraft's stability when the structure is flexible. In this paper, common body coordinate system is utilized to conveniently describe the large deformation and flight dynamics for very flexible flying wing. Small disturbance hypothesis is adopted to establish the stability analysis model. The rigid/elastic motions coupling stability analysis results indicate that the difference between the rigid mode frequency and the elastic mode frequency tends to be unclear when the structural flexibility is significant. This may induce rigid/elastic motion coupling instability problems.

1 INTRODUCTION

For very flexible flying wing, which are sensitive to aerodynamic loads and deformations, analyzing aeroelastic and flight dynamics is quite important in the primary design stage. The extreme length and low stiffness of the wings result in natural vibration frequencies on the order of the flight dynamics such that the aircraft experiences instability characterized by the interaction between the vehicle flight dynamics and the structural vibrations[1]. Therefore, the aeroelastic analysis of these flight vehicles results in aeroelastic mode shapes that have strong components of wing vibration and vehicle body motion. This is the typical rigid/elastic coupling stability problems for very flexible aircrafts, which should consider the flight dynamic feature and aeroelastic feature simultaneously.

Early work addressing flexible wing structural flight dynamics and aeroelasticity was performed by Van Schoor and von Flotow[2]. Their results demonstrated the critical importance of considering the aircraft structural dynamics when analyzing the aircraft flight dynamics of very flexible aircraft [3]. The flight dynamics and aeroelasticity should be analyzed in a unified framework, as suggested by Friedmann[4], Livne and Weisshaar [5], and Livne [6]. Waszak and Schmidt[7] [8]utilized an energy method to establish the dynamic equations for elastic aircraft based on the mean axis, including those for the aircraft's rigid motion and elastic vibration mode. More recently, Hodges[9], Patil[10] and Cesnik [11][12]focused on analyzing the nonlinear aeroelasticity and flight dynamics of flexible aircraft. Their work [13] revealed a significant difference between the short-period and phugoid modes of a very flexible aircraft compared to those of rigid-body, linear aeroelastic,

and nonlinear aeroelastic dynamics. However, most of the researches are based on the nonlinear beam[14] element, which is not convenient for modeling and analyzing in industry. The rigid/elastic coupling stability analysis for engineering application need further study.

The objective of this paper is to establish a state space model via flight dynamic equations based on common body coordinate to analyze the nonlinear flight dynamics and stability characteristic of flexible flying wing. Based on the small disturbance hypothesis, the equations for stability analysis can be greatly simplified. Therefore, it is convenient for researchers to investigate and understand the special characteristics of flexible aircraft. In a simple flying wing example, state space model is used to analyze the differences between the dynamic stability characteristics to illustrate the significant stability problems caused by the rigid/elastic coupling of a very flexible flying wing.

2 THEORETICAL DEVELOPMENT

2.1 Structural Geometric Nonlinearity

The structural geometric nonlinearity roots form the nonlinear geometric equation, which includes the quadric term of the displacement differential, and requires the nonlinear force equilibrium equation established on the deformed state of the structure. The structural geometrically nonlinear problem in this study is solved by ULF[16] method, and the primary equations are presented briefly below.

The relationship between the nonlinear Lagrange/Green strain and displacement is

$${}^t\varepsilon_{ij} = \frac{1}{2}({}^t u_{i,j} + {}^t u_{j,i} + {}^t u_{k,i} {}^t u_{k,j}) \quad (1)$$

where ${}^t u_{i,j}$ is the partial derivative of displacement component u_i to coordinate x_j at time t .

Despite a large elastic deformation, the material remains within the elastic limitation for a small strain, and thus, the conjugate Kirchhoff stress tensor S_{ji} at time t satisfies

$${}^t S_{ji} {}^t n_j {}^t ds = {}^t x_{i,j} {}^t dT_j \quad (2)$$

where ${}^t n_j$ is the direction cosine of a small area element ds at time t , and dT_j is the corresponding surface force in which the follower force effect is considered.

Thus the final element-governing equation can be expressed as[17]:

$$({}^t \mathbf{K}_L + {}^t \mathbf{K}_{NL})\mathbf{u} = {}^{t+\Delta t} \bar{\mathbf{Q}} - {}^t \mathbf{F}_A \quad (3)$$

where ${}^{t+\Delta t} \bar{\mathbf{Q}}$ is the incremental outer force, including the aerodynamic force, engine thrust, and gravity at the new time step. The stiffness matrix in Eq.(3) can be decomposed into a linear part ${}^t \mathbf{K}_L$ and nonlinear part ${}^t \mathbf{K}_{NL}$.

The assumption of a small amplitude vibration around the static equilibrium state is suitable for many dynamic problems, including the dynamic stability of flexible aircraft:

$$\mathbf{u} = \bar{\mathbf{u}} + \mathbf{x} \quad (4)$$

where $\bar{\mathbf{u}}$ is the large-deflect equilibrium deformation from Eq.(3), and \mathbf{x} is a small-vibration deformation. According to Eq. (4) and the static equilibrium condition, the linearized structural quasi-mode can be obtained by generalized diagonalization, and the vibration equation of the system under steady forces reduces to

$$\mathbf{M}_T \ddot{\mathbf{x}} + \mathbf{K}_T \mathbf{x} = 0 \quad (5)$$

where \mathbf{M}_T is the inertial matrix of the structure at the nonlinear static equilibrium configuration, and \mathbf{K}_T is the corresponding stiffness matrix. Both of these parameters are

nonlinear functions of $\bar{\mathbf{u}}$ and vary under different equilibrium states, which is a key feature of geometric nonlinear structures. The mode shapes and frequencies under different equilibrium states can be deduced from Eq.(5).

2.2 Rigid/Elastic Coupling Dynamic Equation

This paper uses the flat geodetic reference frame ($OXYZ$) as the inertial frame and the common body coordinate system ($oxyz$) as the body-reference frame. The origin of the body-reference axes is constrained to an arbitrary pointed position in structure. For the symmetric longitudinal case we will discuss, we define the ox axis along the undeformed airframe pointing towards the back, and the oy axis vertical to the longitudinal symmetry plane of the undeformed aircraft pointing to the right. Figure 1 shows the relationship and position of the two-frame system.

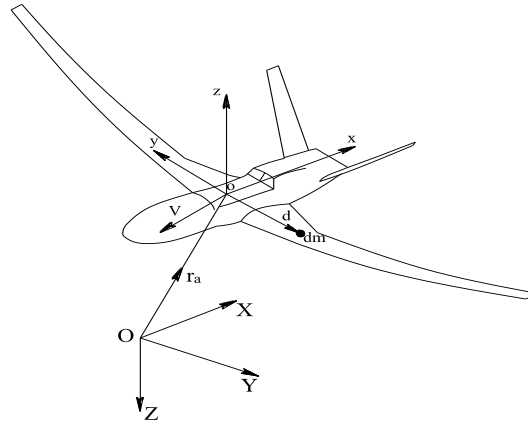


Figure 1. Inertial and body-reference frames

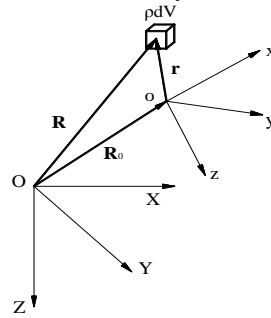


Figure 2. The position of the mass elements under two coordinate frames

The position of an arbitrary mass element of an elastic aircraft can be written in terms of its position relative to the local reference system $oxyz$ and the position of this local reference system relative to the inertial reference frame $OXYZ$. If the body-reference axes $oxyz$ are translating and rotating relative to inertial space with velocity \mathbf{V} and angular velocity $\boldsymbol{\omega}$ and if the position in the mean axes frame can be expressed by the original position \mathbf{r} and deformation \mathbf{u} (i.e., $\mathbf{R} = \mathbf{R}_0 + \mathbf{r} + \mathbf{u}$), then the absolute velocity of the mass element is

$$\begin{aligned}
 \frac{d\mathbf{R}}{dt} &= \frac{d\mathbf{R}_0}{dt} + \frac{d(\mathbf{r} + \mathbf{u})}{dt} \\
 &= \mathbf{v}_0 + \boldsymbol{\omega} \times (\mathbf{r} + \mathbf{u}) + \frac{\delta(\mathbf{r} + \mathbf{u})}{\delta t} \\
 &= \mathbf{v}_0 + (\tilde{\mathbf{r}} + \tilde{\mathbf{u}})^T \boldsymbol{\omega} + \dot{\mathbf{u}}
 \end{aligned} \tag{6}$$

The kinetic energy of the body can be written

$$T = \frac{1}{2} \int_m [\mathbf{v}_o + \boldsymbol{\omega} \times (\mathbf{r} + \mathbf{u}) + \dot{\mathbf{u}}] [\mathbf{v}_o + \boldsymbol{\omega} \times (\mathbf{r} + \mathbf{u}) + \dot{\mathbf{u}}] dm \quad (7)$$

The expended kinetic energy expression is complicated but it can well reflect the kinetic and dynamic characteristics of very flexible aircraft under large deformation. The gravity force can be treated as out force and the elastic potential energy is only related with elastic deformation \mathbf{u} .

As expressed in the body-reference frame, \mathbf{R}, \mathbf{V} and $\boldsymbol{\omega}$ are defined as $\mathbf{R} = [X_m \ Y_m \ Z_m]^T$, $\mathbf{V} = [u \ v \ w]^T$ and $\boldsymbol{\omega} = [p \ q \ r]^T$, respectively. The usual Euler angles $\boldsymbol{\theta} = [\phi \ \theta \ \psi]^T$ are used to define the rotational relationship between the inertial axes and body-reference axes, which is consistent with the analysis of rigid aircraft. The vector $\boldsymbol{\omega}$ can be written as

$$\mathbf{V} = \frac{d\mathbf{R}_0}{dt} = \dot{\mathbf{R}}_0 + \tilde{\boldsymbol{\omega}}\mathbf{R}_0 \quad (8)$$

If we select \mathbf{R}_0 , $\boldsymbol{\theta}$ and \mathbf{u} as the generalized coordinates of the system, according to Lagrange function we can get

$$\frac{d}{dt} \left(\frac{\partial L}{\partial \dot{\mathbf{R}}_0} \right) - \frac{\partial L}{\partial \mathbf{R}_0} = \mathbf{Q}_{R_0}; \quad \frac{d}{dt} \left(\frac{\partial L}{\partial \dot{\boldsymbol{\theta}}} \right) - \frac{\partial L}{\partial \boldsymbol{\theta}} = \mathbf{Q}_{\theta}; \quad \frac{d}{dt} \left(\frac{\partial \hat{L}}{\partial \dot{\mathbf{u}}} \right) - \frac{\partial \hat{L}}{\partial \mathbf{u}} = \mathbf{Q}_u \quad (9)$$

Substitute kinetic equation and kinetic energy expression into Eq.(9), then we can obtain the translate equation, rotation equation and elastic equation.

$$M\dot{\mathbf{v}}_o + \tilde{\mathbf{S}}^T \dot{\boldsymbol{\omega}} + \int_m \ddot{\mathbf{u}} dm - (M\tilde{\mathbf{v}}_o + \tilde{\boldsymbol{\omega}}\tilde{\mathbf{S}} + 2\tilde{\mathbf{S}}_v) \boldsymbol{\omega} = \mathbf{Q}_{R_0} \quad (10)$$

$$\tilde{\mathbf{S}}\dot{\mathbf{v}}_o + \mathbf{J}_{total} \dot{\boldsymbol{\omega}} + \int_m (\tilde{\mathbf{r}} + \tilde{\mathbf{u}}) \ddot{\mathbf{u}} dm - \left(2 \int_m (\tilde{\mathbf{r}} + \tilde{\mathbf{u}}) \dot{\tilde{\mathbf{u}}} dm + \tilde{\mathbf{S}}\tilde{\mathbf{v}}_o - \tilde{\boldsymbol{\omega}}\mathbf{J}_{total} \right) \boldsymbol{\omega} = (\mathbf{D}^T)^{-1} \mathbf{Q}_{\theta} - \tilde{\mathbf{R}}_o \mathbf{Q}_{R_0} \quad (11)$$

$$\dot{\mathbf{v}}_o dm + (\tilde{\mathbf{r}} + \tilde{\mathbf{u}})^T \dot{\boldsymbol{\omega}} dm + \ddot{\mathbf{u}} dm + (\tilde{\mathbf{v}}_o^T - \tilde{\boldsymbol{\omega}}(\tilde{\mathbf{r}} + \tilde{\mathbf{u}}) + 2\dot{\tilde{\mathbf{u}}}^T) \boldsymbol{\omega} dm + k(\mathbf{u})\mathbf{u} = \mathbf{Q}_u \quad (12)$$

Thus the flight dynamic equation under common body coordinate system for very flexible aircraft is obtained.

$$M\dot{\mathbf{v}}_o + \tilde{\mathbf{S}}^T \dot{\boldsymbol{\omega}} + \int_m \ddot{\mathbf{u}} dm - (M\tilde{\mathbf{v}}_o + \tilde{\boldsymbol{\omega}}\tilde{\mathbf{S}} + 2\tilde{\mathbf{S}}_v) \boldsymbol{\omega} = \mathbf{F}_m$$

$$\tilde{\mathbf{S}}\dot{\mathbf{v}}_o + \mathbf{J}_{total} \dot{\boldsymbol{\omega}} + \int_m (\tilde{\mathbf{r}} + \tilde{\mathbf{u}}) \ddot{\mathbf{u}} dm - \left(2 \int_m (\tilde{\mathbf{r}} + \tilde{\mathbf{u}}) \dot{\tilde{\mathbf{u}}} dm + \tilde{\mathbf{S}}\tilde{\mathbf{v}}_o - \tilde{\boldsymbol{\omega}}\mathbf{J}_{total} \right) \boldsymbol{\omega} = \mathbf{M}_m \quad (13)$$

$$\dot{\mathbf{v}}_o dm + (\tilde{\mathbf{r}} + \tilde{\mathbf{u}})^T \dot{\boldsymbol{\omega}} dm + \ddot{\mathbf{u}} dm + (\tilde{\mathbf{v}}_o^T - \tilde{\boldsymbol{\omega}}(\tilde{\mathbf{r}} + \tilde{\mathbf{u}}) + 2\dot{\tilde{\mathbf{u}}}^T) \boldsymbol{\omega} dm + k(\mathbf{u})\mathbf{u} = \mathbf{Q}_u$$

According to the virtual work principle, the generalized force can be expressed as,

$$\mathbf{F}_m = \mathbf{Q}_{R_0} = \int_V \mathbf{f} dV \quad (14)$$

$$\mathbf{M}_m = (\mathbf{D}^T)^{-1} \mathbf{Q}_{\theta} - \tilde{\mathbf{R}}_o \mathbf{Q}_{R_0} = \int_V (\tilde{\mathbf{r}} + \tilde{\mathbf{u}}) \mathbf{f} dV$$

These equations demonstrate that \mathbf{F}_m is the total external force acting on the elastic structure in the body-reference frame and that \mathbf{M}_m is the total external moment in the body-reference frame. The generalized force includes gravity \mathbf{G} aerodynamic force \mathbf{A} and the engine thrust \mathbf{T} .

To express the specific location of the aircraft in the inertial frame, \mathbf{R} can be written as $\mathbf{R}=[X_E \ Y_E \ Z_E]^T$ in the inertial frame. Thus, the translate velocity of cg can be expressed by the cg position in space via common translation matrix.

$$\dot{\mathbf{R}} = \mathbf{L}^T \mathbf{V} \quad (15)$$

In general, the kinetic equations can be expressed as

$$\begin{aligned} \dot{\mathbf{R}} &= \mathbf{L}^T \mathbf{V} \\ \dot{\boldsymbol{\theta}} &= \mathbf{D}^{-1} \boldsymbol{\omega} \end{aligned} \quad (16)$$

Introduce rigid motion mode (Φ_t for translate motion and Φ_r for rotation mode) into common body coordinate system. With the grid force expression, the final rigid/elastic coupling dynamic equations are

$$\begin{aligned} M\dot{\mathbf{v}}_o + \tilde{\mathbf{S}}^T \dot{\boldsymbol{\omega}} + \int_m \ddot{\mathbf{u}} dm - (M\tilde{\mathbf{v}}_o + \tilde{\boldsymbol{\omega}}\tilde{\mathbf{S}} + 2\tilde{\mathbf{S}}_v) \boldsymbol{\omega} &= \Phi_t^T (\mathbf{f}_G + \mathbf{f}_A + \mathbf{f}_T) \\ \tilde{\mathbf{S}}\dot{\mathbf{v}}_o + \mathbf{J}_{total} \dot{\boldsymbol{\omega}} + \int_m (\tilde{\mathbf{r}} + \tilde{\mathbf{u}}) \ddot{\mathbf{u}} dm - \left(2 \int_m (\tilde{\mathbf{r}} + \tilde{\mathbf{u}}) \dot{\mathbf{u}} dm + \tilde{\mathbf{S}}\dot{\mathbf{v}}_o - \tilde{\boldsymbol{\omega}}\mathbf{J}_{total} \right) \boldsymbol{\omega} &= \Phi_r^T (\mathbf{f}_G + \mathbf{f}_A + \mathbf{f}_T) \\ \dot{\mathbf{v}}_o dm + (\tilde{\mathbf{r}} + \tilde{\mathbf{u}})^T \dot{\boldsymbol{\omega}} dm + \ddot{\mathbf{u}} dm + (\tilde{\mathbf{v}}_o^T - \tilde{\boldsymbol{\omega}}(\tilde{\mathbf{r}} + \tilde{\mathbf{u}}) + 2\tilde{\mathbf{u}}^T) \boldsymbol{\omega} dm + k(\mathbf{u})\mathbf{u} &= f_G + f_A + f_T \\ \dot{\mathbf{R}} &= \mathbf{L}^T \mathbf{V} \\ \dot{\boldsymbol{\theta}} &= \mathbf{D}^{-1} \boldsymbol{\omega} \end{aligned} \quad (17)$$

The equilibrium equations for static aeroelastic analysis under quasi-steady assumption can be obtained. Geometrically nonlinear trim analysis can be executed with Eq.(18).

$$\begin{aligned} M\tilde{\mathbf{v}}_o + \tilde{\mathbf{S}}^T \dot{\boldsymbol{\omega}} - M\tilde{\mathbf{v}}_o \boldsymbol{\omega} - \tilde{\boldsymbol{\omega}}\tilde{\mathbf{S}}\boldsymbol{\omega} &= \Phi_t^T (\mathbf{f}_G + \mathbf{f}_A + \mathbf{f}_T) \\ \tilde{\mathbf{S}}\dot{\mathbf{v}}_o + \mathbf{J}\dot{\boldsymbol{\omega}} - \tilde{\mathbf{S}}\dot{\mathbf{v}}_o \boldsymbol{\omega} + \tilde{\boldsymbol{\omega}}\mathbf{J}\boldsymbol{\omega} &= \Phi_r^T (\mathbf{f}_G + \mathbf{f}_A + \mathbf{f}_T) \\ \dot{\mathbf{v}}_o dm + (\tilde{\mathbf{r}} + \tilde{\mathbf{u}})^T \dot{\boldsymbol{\omega}} dm + (\tilde{\mathbf{v}}_o^T - \tilde{\boldsymbol{\omega}}(\tilde{\mathbf{r}} + \tilde{\mathbf{u}})) \boldsymbol{\omega} dm + k\mathbf{u} &= f_G + f_A + f_T \end{aligned} \quad (18)$$

2.3 Rigid/Elastic Coupling State Space Modeling and Stability Analysis

Considering the geometrically nonlinear large structural deformation, the nonlinear trimmed state is selected as a benchmark state for stability analysis. Then the existed large deflection under trim state can be expressed as frozen deformation \mathbf{r} in common body coordinates to represent the variation of cg and rotational inertia. Thus the small elastic deformation around equilibrium state can be expressed with mode obtained via Eq. (5).

$$\mathbf{u}(\mathbf{r}, t) = \sum_{i=1}^n q_i(t) \boldsymbol{\psi}_i(\mathbf{r}) = \boldsymbol{\psi}(\mathbf{r}) \mathbf{q}(t) \quad (19)$$

Then the Eq.(18) can be rewritten in matrix form as[18],

$$\begin{bmatrix} M\mathbf{I} & -M\tilde{\mathbf{r}}_G & \mathbf{P} \\ M\tilde{\mathbf{r}}_G & \mathbf{J} & \mathbf{H} \\ \mathbf{P}^T & \mathbf{H}^T & \mathbf{M} \end{bmatrix} \begin{bmatrix} \dot{\mathbf{v}}_0 \\ \dot{\boldsymbol{\omega}} \\ \dot{\mathbf{q}} \end{bmatrix} + \begin{bmatrix} M\tilde{\boldsymbol{\omega}} & -M\tilde{\boldsymbol{\omega}}\tilde{\mathbf{r}}_G & 2\mathbf{P}_{\dot{q}} \\ M\tilde{\mathbf{r}}_G \tilde{\boldsymbol{\omega}} & \tilde{\boldsymbol{\omega}}\mathbf{J} & 2\mathbf{H}_{\dot{q}} \\ -\mathbf{P}_{\dot{q}}^T & -\mathbf{H}_{\dot{q}}^T & 2\mathbf{M}_{\dot{q}} \end{bmatrix} \begin{bmatrix} \mathbf{v}_0 \\ \boldsymbol{\omega} \\ \dot{\mathbf{q}} \end{bmatrix} + \begin{bmatrix} \mathbf{0} \\ \mathbf{0} \\ \mathbf{Kq} \end{bmatrix} = \begin{bmatrix} \mathbf{F}_m \\ \mathbf{M}_m \\ \mathbf{Q}_u \end{bmatrix} \quad (20)$$

Select the straight flight state as benchmark to linearize Eq.(20) by small disturbance assumption, then $\mathbf{v}_o = (u_0, 0, 0)$, $\dot{\mathbf{v}}_o = \boldsymbol{\omega}_0 = \dot{\boldsymbol{\omega}}_0 = \dot{\boldsymbol{\theta}}_0 = 0$, $(\phi_0 \ \theta_0 \ \psi_0) = (0 \ 0 \ 0)$ $\dot{\mathbf{q}} = \mathbf{0}$. For stability analysis, the elastic deformation caused by small disturbance is quite small. The configuration and cg almost remain unchanged. Thus the center of common body coordinates

can be transferred to the cg of benchmark state, in which the large deflections have already been considered. Then the simplified dynamic equations for stability analysis are[18],

$$\begin{bmatrix} \mathbf{M}\mathbf{I} & \mathbf{0} & \mathbf{0} \\ \mathbf{0} & \mathbf{J} & \mathbf{0} \\ \mathbf{0} & \mathbf{0} & \mathbf{M} \end{bmatrix} \begin{bmatrix} \Delta\dot{\mathbf{v}}_0 \\ \Delta\dot{\boldsymbol{\omega}} \\ \Delta\dot{\mathbf{q}} \end{bmatrix} + \begin{bmatrix} \mathbf{0} & -M\tilde{\mathbf{v}}_0 & \mathbf{0} \\ \mathbf{0} & \mathbf{0} & \mathbf{0} \\ \mathbf{0} & \mathbf{0} & \mathbf{0} \end{bmatrix} \begin{bmatrix} \Delta\mathbf{v}_0 \\ \Delta\boldsymbol{\omega} \\ \Delta\dot{\mathbf{q}} \end{bmatrix} + \begin{bmatrix} \mathbf{0} \\ \mathbf{0} \\ \mathbf{K}\Delta\mathbf{q} \end{bmatrix} = \begin{bmatrix} \Delta\mathbf{F} \\ \Delta\mathbf{M} \\ \Delta\mathbf{Q} \end{bmatrix} \quad (21)$$

As for the unsteady aerodynamic modeling, nonplanar doublet lattice method and rational function fitting strategy are utilized as routine. So here we give the final aerodynamic model results.

$$\Phi_S \mathbf{f}_A(t) = q_\infty [(A_{SS0} \mathbf{q}_S + A_{SC0} \boldsymbol{\delta}) + \frac{L}{V_\infty} (A_{SS1} \dot{\mathbf{q}}_S + A_{SC1} \dot{\boldsymbol{\delta}}) + \frac{L^2}{V_\infty^2} (A_{SS2} \ddot{\mathbf{q}}_S + A_{SC2} \ddot{\boldsymbol{\delta}}) + D \mathbf{x}_a(s)] \quad (22)$$

Now we can rewritten Eq.(21) as[18]

$$\begin{aligned} \mathbf{M}_S \dot{\mathbf{V}}_S + \mathbf{B}_S \mathbf{V}_S + \mathbf{K}_S \mathbf{R}_S &= q_\infty (A_{SS0} \mathbf{L}_{R0} + \frac{C_{ref}}{2V_\infty} A_{SS1} \mathbf{L}_{R1}) \mathbf{R}_S + q_\infty \frac{C_{ref}}{2V_\infty} A_{SS1} \mathbf{V}_S \\ &+ q_\infty \frac{C_{ref}^2}{4V_\infty^2} A_{SS2} \dot{\mathbf{V}}_S + q_\infty A'_{SC0} \boldsymbol{\delta} + q_\infty \frac{C_{ref}}{2V_\infty} A_{SC1} \dot{\boldsymbol{\delta}} + (-\mathbf{M}_C + q_\infty \frac{C_{ref}^2}{4V_\infty^2} A_{SC2}) \ddot{\boldsymbol{\delta}} + q_\infty D \mathbf{x}_a \end{aligned} \quad (23)$$

$$\text{Where } \mathbf{M}_S = \begin{bmatrix} \mathbf{M}\mathbf{I}_3 & & \\ & \mathbf{I} & \\ & & \mathbf{M}_{ee} \end{bmatrix} \mathbf{K}_S = \begin{bmatrix} \mathbf{0}_{3 \times 3} & -M\mathbf{T}_g & \\ & \mathbf{0}_{3 \times 3} & \\ & -\mathbf{M}_{eg} \mathbf{T}_g & \mathbf{K}_{ee} \end{bmatrix} \mathbf{B}_S = \begin{bmatrix} \mathbf{0}_{3 \times 3} & -M\tilde{\mathbf{V}}_0 & \\ & \mathbf{0}_{3 \times 3} & \\ & & \mathbf{B}_{ee} \end{bmatrix} \mathbf{M}_C = \begin{bmatrix} \mathbf{0}_{3 \times nc} \\ \mathbf{0}_{3 \times nc} \\ \mathbf{M}_{ec} \end{bmatrix}$$

Converting Eq.(23) into state space we can get[18]

$$\begin{aligned} \dot{\mathbf{x}}_{ae} &= \mathbf{A}_{ae} \mathbf{x}_{ae} + \mathbf{B}_{ae} \boldsymbol{\eta} \\ \mathbf{x}_{ae} &= \begin{bmatrix} \mathbf{R}_S \\ \mathbf{V}_S \\ \mathbf{x}_a \end{bmatrix} \mathbf{A}_{ae} = \begin{bmatrix} \mathbf{L}_{S0} & \mathbf{L}_{S1} & \\ \bar{\mathbf{K}}_S & \bar{\mathbf{B}}_S & \bar{D} \\ E_S \mathbf{L}_{R1} & E_S & \bar{R}_a \end{bmatrix} \\ \boldsymbol{\eta} &= \begin{bmatrix} \boldsymbol{\delta} \\ \dot{\boldsymbol{\delta}} \\ \ddot{\boldsymbol{\delta}} \end{bmatrix} \mathbf{B}_{ae} = \begin{bmatrix} \mathbf{0}_{ns \times nc} & & \\ \bar{\mathbf{K}}_C & \bar{\mathbf{B}}_C & \bar{\mathbf{M}}_C \\ & E_c & \mathbf{0}_{nr \times nc} \end{bmatrix} \end{aligned} \quad (24)$$

$$\bar{\mathbf{M}}_S = (\mathbf{M}_S - q_\infty \frac{C_{ref}^2}{4V_\infty^2} A_{SS2})^{-1} \quad \bar{\mathbf{M}}_C = \bar{\mathbf{M}}_S (-\mathbf{M}_C + q_\infty \frac{C_{ref}^2}{4V_\infty^2} A_{SC2})$$

$$\text{Where } \bar{\mathbf{B}}_S = -\bar{\mathbf{M}}_S (\mathbf{B}_S - q_\infty \frac{C_{ref}}{2V_\infty} A_{SS1}) \quad \bar{\mathbf{B}}_C = q_\infty \frac{C_{ref}}{2V_\infty} \bar{\mathbf{M}}_S A_{SC1}$$

$$\bar{\mathbf{K}}_S = -\bar{\mathbf{M}}_S (\mathbf{K}_S - q_\infty A_{SS0} \mathbf{L}_{R0} - q_\infty \frac{C_{ref}}{2V_\infty} A_{SS1} \mathbf{L}_{R1}) \quad \bar{\mathbf{K}}_C = q_\infty \bar{\mathbf{M}}_S A_{SC0}$$

$$\bar{D} = q_\infty \bar{\mathbf{M}}_S D \quad \bar{R}_a = \frac{2V_\infty}{C_{ref}} R_a$$

By analyzing the eigenvalues and eigenvectors of Eigen matrix \mathbf{A}_{ae} , the stability characteristics can be obtained. The rigid/elastic coupling dynamic state space modeling

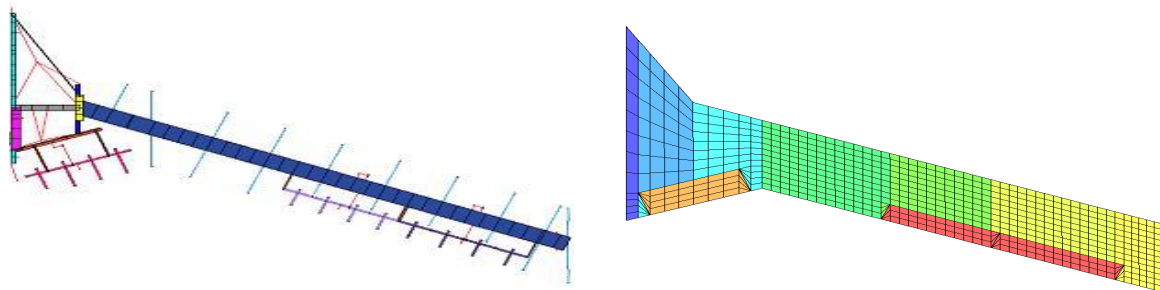
above is derived from the large nonlinear deformation of elastic aircraft based on common body coordinate system. It well meets the demand of rigid/elastic coupling stability analysis under large deformation for very flexible aircraft.

3 EXAMPLE

Here gives a small analysis example in order to illustrate the theoretical modeling process and verify the applicability of the method established in this paper.

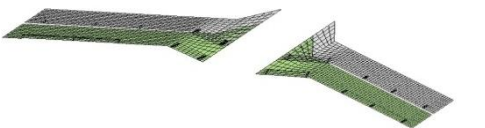
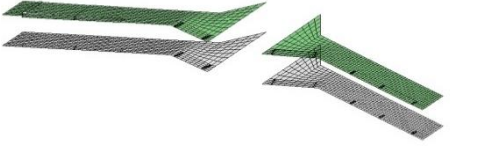
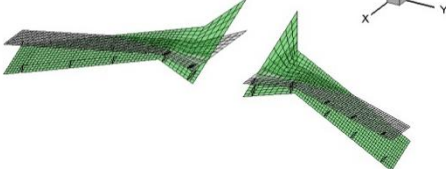
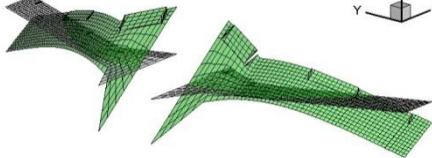
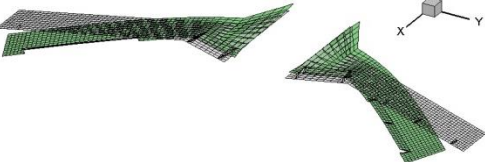
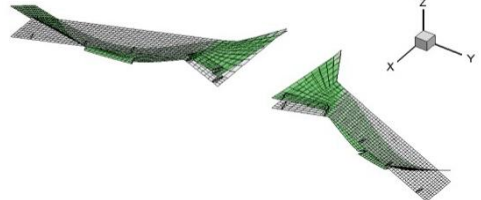
3.1 Flying Wing

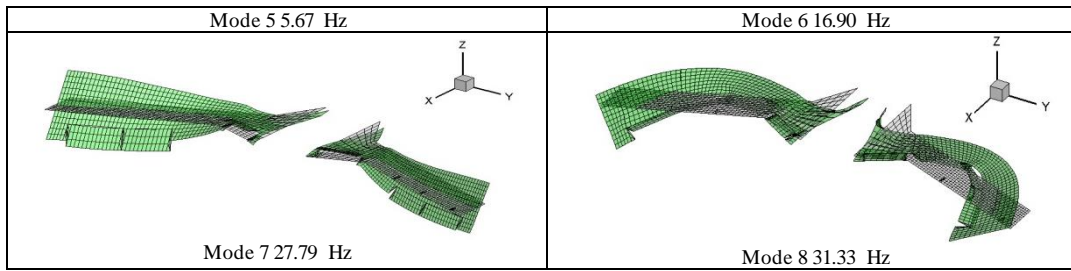
The flying wing model used in this paper is a wind tunnel test semi-model, shown in Figure 3. In order to present the special coupled stability problem, the complete model is utilized to analyze the longitudinal coupled stability. There are two control surfaces at the tailing edge of each wing and one control surface at the trailing edge of fuselage. Considering the longitudinal symmetric flight condition, the outer control surfaces at each wing are defined as the elevators and others keep stable. The FEM model of the flying wing is constructed with beam elements and concentrate mass elements. Nonplanar Doublet lattice panel method is used to establish the aerodynamic modeling for flying wing. For longitudinal flight analysis, the three DOFs of side motion, roll and yaw are the constraints at the instantaneous center of gravity. 3 rigid modes and 7 symmetric elastic modes are utilized in stability analysis and the detailed information are shown in Table 1.



a. structure model b. aerodynamic model
Figure 3. Flying wing semi-model

Table 1 Mode information used in stability analysis

 <p>Mode 1 0.00 Hz</p>	 <p>Mode 2 0.00 Hz</p>
 <p>Mode 3 0.00 Hz</p>	 <p>Mode 4 5.08 Hz</p>
	



3.2 Nonlinear Coupled Stability Analysis

The longitude stability characteristics under 1 g straight flight are discussed below. The nonlinear stability analysis was linearized at each nonlinear equilibrium state. In the rigid/elastic coupling state space modeling analysis, 3 rigid longitudinal motion modes (moving forward, plunging, and pitching) and 7 elastic vibration modes (Table 1) were selected. One lagging root was used to establish the rigid/elastic coupling state space model. By solving the eigenvalue of Eigen matrix A_{ae} , the root locus of eigenvalue vs. flight speed can be obtained to determine the stability of the system. For comparison, the traditional flutter analysis was also implemented. The 3 rigid modes were included and treated as normal modes since the traditional flutter analysis cannot consider about the nonlinear coupling effects.

The flutter analysis results obtained by pk method are shown in Figure 4. For clearance, only three modes that participated in the flutter are shown in the figure, which indicates that the pitching mode and bend mode tend to be coupled together and result in the critical flutter speed 36.5m/s.

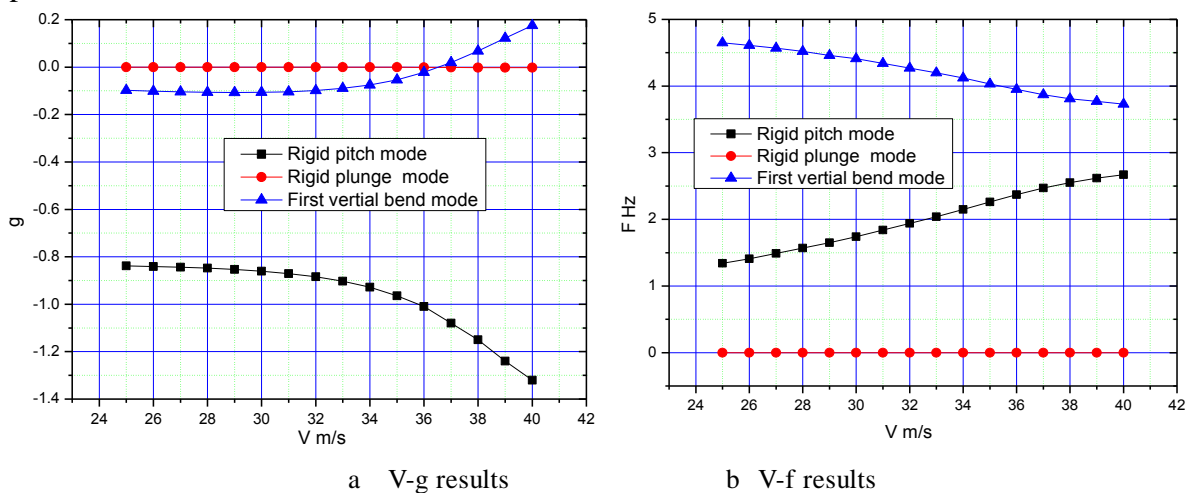


Figure 4 Flutter analysis results

The nonlinear coupled stability analysis was implemented in time domain via state space model established in this paper. The obtained results are shown in Figure 5. The develop trend of each mode along with the increase in flight speed is marked with a black arrow; the critical speed crossing the imaginary axis is marked with a red arrow. The mode 4 (vertical wing bend mode referenced in Table 1) cross the imaginary axis within the calculation range and results in the nonlinear coupled critical speed 32m/s. The Eigen vector of mode 4 at critical speed is shown in Figure 6. It can be clearly identified that the coupled pitching mode and wing bend mode makes the flying wing unstable, which is similar with the flutter results. However, the nonlinear coupled result is lower than the flutter results. This is because the flutter analysis can not reflect the dynamic coupling effect of flexible aircrafts. All modes have no mass inertial coupling and dynamic coupling. While in nonlinear analysis, the

complicated dynamic coupling effects are considered and the structural geometric nonlinearity is included. Since the state space model is linearized under different equilibrium stats, the obtained quasi-modes are varied. The frequency decline of wing bend make it closer to the rigid mode frequency and easier coupled with rigid mode. So the nonlinear dynamic coupled stability analysis is more close to reality and more reliable.

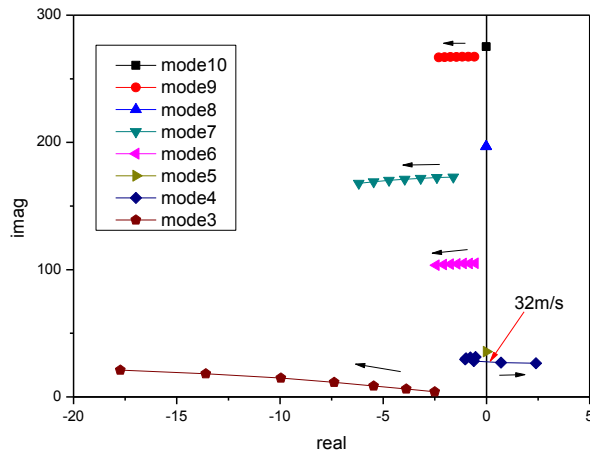


Figure 5 Nonlinear coupled analysis results

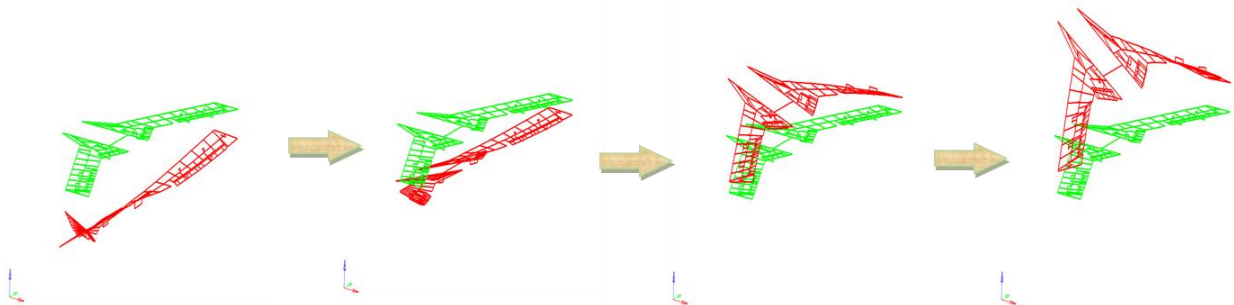


Figure 6 Unstable mode

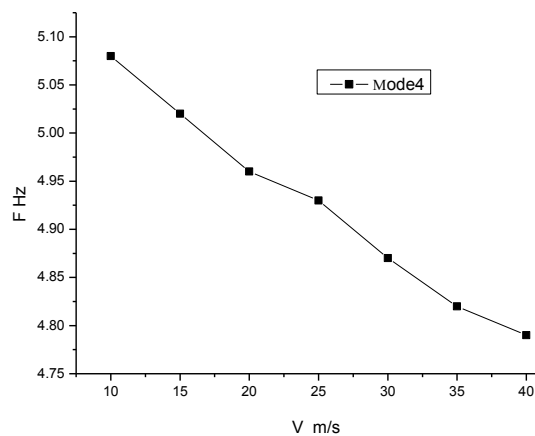


Figure 7 Frequency of mode 4 under different speed.

4 CONCLUSION

A theoretical nonlinear rigid/elastic coupling stability analysis state space model is established in this paper. For easy implementation and intuitionistic understandings, the small turbulence hypothesis is adopted for stability analysis. By transferring the center of common body system to the center of gravity under nonlinear large deformed equilibrium configuration, the inertia coupling can be eliminated for rigid/elastic stability analysis. A

flexible flying wing is selected as an example to illustrate the special rigid/elastic coupling stability characteristics. The rigid/elastic coupling instability becomes the main reason that seriously affects the aircraft's envelope. The comparison of flutter analysis and nonlinear analysis results indicates that the structural geometric nonlinearity caused by large deformation may worsen the rigid/elastic coupling instability. Thus, for flexible flying wing, the geometrically nonlinear rigid/elastic coupling is inevitable in determining the aircraft envelope. The theoretical analysis model established in this paper is an acceptable way to analyze the special stability characteristics for flexible aircraft.

5 REFERENCES

- [1] Richards, P. W., Mardanpour, P., Herd, R. A., and Hodges, D. H. Effect of Inertial and Constitutive Properties on Body-Freedom Flutter of a Flying Wing. 54th AIAA/ASME/ASCE/AHS/ASC Structures, Structural Dynamics, and Materials Conference, Apr. 8-11, 2013, AIAA, Boston, pp. 2013-1840.
- [2] Van Schoor, M. C. and von Flotow, A. H. Aeroelastic Characteristics of a Highly Flexible Aircraft. *Journal of Aircraft*, Vol. 27, No. 10, 1990, pp. 901-908. doi: 10.2514/3.45955
- [3] Shearer, C. M., and Cesnik, C. E. S. Nonlinear Flight Dynamics of Very Flexible Aircraft. *Journal of Aircraft*, Vol. 44, No. 5, 2007, 1528-1545. doi: 10.2514/1.27606
- [4] Friedmann, P. P. Renaissance of Aeroelasticity and Its Future. *Journal of Aircraft*, Vol. 36, No. 1, 1999, pp. 105-121. doi: 10.2514/2.2418
- [5] Livne, E., and Weisshaar, T. A. Aeroelasticity of Nonconventional Airplane Configurations-Past and Future. *Journal of Aircraft*, Vol. 40, No. 6, 2003, pp. 1047-1065. doi: 10.2514/2.7217
- [6] Livne, E. Future of Airplane Aeroelasticity. *Journal of Aircraft*, Vol. 40, No. 6, 2003, pp. 1066-1092. doi: 10.2514/2.7218
- [7] Waszak, M. R., and Schmidt, D. K. On the Flight Dynamics of Aeroelastic Vehicles. AIAA-86-2077, 1986.
- [8] Waszak, M. R., and Schmidt, D. K. Flight Dynamics of Aeroelastic Vehicles. *Journal of Aircraft*, Vol. 25, No. 6, 1988, 563-571. doi: 10.2514/3.45623
- [9] Patil, M. J., and Hodges, D. H. Flight Dynamics of Highly Flexible Flying Wings. *Journal of Aircraft*, Vol. 43, No. 6, 2006, pp. 1790-1799. doi: 10.2514/1.17640
- [10] Hodges, D. H. Geometrically Exact, Intrinsic Theory for Dynamics of Curved and Twisted Anisotropic Beams. *AIAA Journal*, Vol. 41, No. 6, 2003, pp. 1131-1137. doi: 10.2514/2.2054
- [11] Cesnik, C. E. S., and Su, W. Nonlinear Aeroelastic Modeling and Analysis of Fully Flexible Aircraft. Proceedings of the 46th AIAA/ASME/ASCE/AHS/ASC Structures, Structural Dynamics, and Materials Conference, AIAA Paper 2005-2169, Austin, TX, April 2005.
- [12] Arizono, H., and Cesnik, C. E. S. Computational Static Aeroelasticity Using Nonlinear Structures and Aerodynamics Mo. 54th AIAA/ASME/ASCE/AHS/ASC Structures, Structural Dynamics, and Materials Conference, Boston, April 8-11, 2013.
- [13] Patil, M. J., Hodges, D. H., and Cesnik, C. E. S. Nonlinear Aeroelasticity and Flight Dynamics of High-Altitude Long-Endurance Aircraft. *Journal of Aircraft*, Vol. 38, No. 1, 2001, pp. 88-94; also AIAA Paper 99-1470, 1999. doi: 10.2514/2.2738

- [14] Hodges, D. H., A Mixed Variational Formulation Based on Exact Intrinsic Equations for Dynamics of Moving Beams, *International Journal of Solids and Structures*, Vol. 26, No. 11, 1990, pp. 1253-1273. doi: 10.1016/0020-7683(90)90060-9
- [15] Tianxia, S., *Nonlinear Structure Finite Element Computation*, University of Science & Technology Press, HuaZhong, 1996 (in Chinese).
- [16] Wang, X. C., and Shao, M., *Theory and Numerical Methods of Finite Element Method*, Tsinghua University Press, Beijing, 1997 (in Chinese).
- [17] Xie, C., and Yang, C. Linearization Method of Nonlinear Aeroelastic Stability for Complete Aircraft with High-Aspect-Ratio Wings. *Science China Technological Sciences*, Vol. 54, No. 2, 2011, pp. 403-411. doi: 10.1007/s11431-010-4252-5
- [18] Liu Yi. *Aeroelastic Stability and Response Analysis of Very Flexible Aircraft* Ph.D. dissertation, Beihang University, Beijing, 2016.

COPYRIGHT STATEMENT

The authors confirm that they hold copyright on all of the original material included in this paper. The authors also confirm that they have obtained permission, from the copyright holder of any third party material included in this paper, to publish it as part of their paper. The authors confirm that they give permission, or have obtained permission from the copyright holder of this paper, for the publication and distribution of this paper as part of the IFASD-2017 proceedings or as individual off-prints from the proceedings.